



1 **Temporal changes in photoreactivity of dissolved organic carbon and implications for aquatic**
2 **carbon fluxes from peatlands**

3 Amy E Pickard^{1, 2*}, Kate V Heal¹, Andrew R McLeod¹ and Kerry J Dinsmore²

4 ¹School of GeoSciences, Alexander Crum Brown Rd, Kings Buildings, The University of Edinburgh,
5 UK, EH9 3FF *amy.pickard@ed.ac.uk

6 ²Centre for Ecology & Hydrology, Bush Estate, Penicuik, UK, EH26 0QB

7 **Abstract**

8 Aquatic systems draining peatland catchments receive a high loading of dissolved organic carbon
9 (DOC) from the surrounding terrestrial environment. Whilst photo-processing is known to be an
10 important process in the transformation of aquatic DOC, the drivers of temporal variability in this
11 pathway are less well understood. In this study, laboratory irradiation experiments were conducted on
12 water samples collected from two contrasting peatland aquatic systems in Scotland. The first system
13 was a stream draining the Auchencorth Moss peatland with high DOC concentrations subject to
14 strong seasonal and flow driven variability. The second was the low DOC reservoir, Loch Katrine,
15 also situated in a catchment with a high percentage peat cover. Samples were collected monthly at
16 both sites from May 2014 to May 2015 and from the stream system during two rainfall events. DOC
17 concentrations, absorbance properties and fluorescence characteristics were measured to investigate
18 characteristics of the photochemically labile fraction of DOC. CO₂ and CO produced by irradiation
19 were also measured to determine total photoproduction and intrinsic sample photoreactivity.
20 Significant variation was seen in the photoreactivity of DOC between the two systems, with total
21 irradiation induced changes typically two orders of magnitude greater at the high DOC stream site.
22 This is attributed to longer water residence times in the reservoir rendering a higher proportion of the
23 DOC recalcitrant to photo-processing. Rainfall events were identified as important in replenishing
24 photoreactive material in the stream, with lignin phenol data (Ad:Al_{v,s} and P:V) indicating
25 mobilisation of fresh DOC derived from woody vegetation in the upper catchment. Using DOC-CO₂
26 conversion data from irradiation experiments, we estimate that the contribution of Auchencorth Moss



27 catchment to photo-induced aquatic CO₂ production is up to 3.48 ± 2.02 kg CO₂ yr⁻¹. We have shown
28 that peatland catchments produce significant volumes of aromatic DOC and that photoreactivity of
29 this DOC is greatest in the headwaters, however an improved understanding of water residence times
30 and DOC input-output along the source to sea aquatic pathway is required to determine the fate of
31 peatland carbon.

32 **Keywords:** Carbon budgets ▪ Rainfall events ▪ Lignin phenols

33 1. Introduction

34 DOC is transported from terrestrial environments to aquatic systems where it plays an important role
35 in carbon (C) cycling. Biogeochemical transformations of DOC via microbial and photochemical
36 pathways impact significantly on aquatic C cycles, with up to 55% of C exported as DOC to
37 freshwaters estimated to be lost to the atmosphere as CO₂ (Cole et al., 2007; Tranvik et al., 2009;
38 Cory et al., 2014). These estimates suggest that the C sink strength of the land surface globally has
39 been overestimated, as the role of freshwater systems in the biogeochemical processing of DOC and
40 the subsequent production of greenhouse gases had not been considered. Understanding of the rate of
41 turnover of DOC in aquatic systems remains incomplete and further efforts are required to quantify
42 the extent to which biogeochemical processes in aquatic systems are a source of C to the atmosphere.

43 Photochemical reactions in aquatic systems are induced by the absorption of solar radiation,
44 particularly in the UV region of the spectrum, and preferentially affect aromatic, high molecular
45 weight (HMW) molecules derived from allochthonous sources. Upon radiation, HMW DOC is
46 converted to microbially available low molecular weight (LMW) carbon substrates (Opsahl and
47 Benner, 1998; Sulzberger and Durisch-Kaiser, 2009). Photodegradation of DOC also results in the
48 production of C based gases, primarily CO₂ and CO (Stubbins et al., 2011). Whilst it is understood
49 that input of photochemically labile terrigenous DOC can regulate C cycling in aquatic systems (Cory
50 et al., 2014; Koehler et al., 2014), the significance of DOC photodegradation processes in these cycles
51 remains poorly constrained over time and space (Franke et al., 2012; Moody et al., 2013). Due to low
52 temperatures and short residence times limiting autochthonous (in situ) DOC production in headwater



53 systems of northern peatlands, photochemical processing may be a proportionately more important
54 process.

55 A key control on DOC concentrations in headwater systems is rainfall events which flush young, less
56 degraded plant material within the catchment into streams (Evans et al., 2007; Austnes et al., 2010).
57 Rainfall events have been shown to contribute significantly to annual C export from peatland
58 headwater streams (Clark et al., 2007), yet the degree to which they replenish photolabile material
59 within the aquatic environment is less certain. Stormflows in northern catchments have been
60 associated with increased contribution of humic like material (Fellman et al., 2009), suggesting that
61 DOC photoreactivity may also increase during these events. Several studies have explored seasonal
62 variation in intrinsic DOC photoreactivity in northern aquatic systems (Vachon et al., 2016; Franke et
63 al., 2012) yet, to our knowledge, the contribution of rainfall events to the seasonal cycle of photolabile
64 material has not been previously investigated.

65 Further uncertainty remains in understanding the variation in DOC photolability at different positions
66 within a watershed (Franke et al. 2012). The increasing residence time of downstream aquatic
67 systems, as headwater streams drain into rivers, lacustrine and marine environments, may mean that
68 photo-processing becomes a more important control on overall C budgets with distance downstream.
69 Conversely, the extent to which the material has already been degraded in the upstream aquatic
70 environment may mean that further processing is limited (Catalán et al., 2016; Vähätalo and Wetzel,
71 2008). Investigating the susceptibility of DOC to photo-processing in different types of aquatic
72 environments will allow the overall contribution of photochemical processes to C cycling to be
73 understood on a catchment scale.

74 The primary aim of this study was to assess temporal variation in the photochemical lability of DOC
75 from two contrasting aquatic systems draining peatlands and to understand how this variation may
76 impact aquatic C budgets. Controlled UV irradiation experiments were conducted on water samples
77 collected from the two contrasting aquatic systems, one a stream and the other a reservoir. Water from
78 both systems was sampled on a monthly basis over a 1 year period and also from the high DOC



79 stream system during two rainfall events to characterise short term variability in DOC concentration
80 and composition. After experimental exposure, optical, spectroscopic and biogeochemical analyses of
81 the water samples were conducted to explore DOC photoreactivity and the resultant production of C
82 based gases. The results were used to test the following hypotheses:

83 H1: Both aquatic systems will exhibit seasonality with regards to the supply of photochemically labile
84 DOC, with highest photolability detected in the winter due to limited processing in the aquatic
85 environment.

86 H2: Photochemical degradation of DOC will be a more significant loss term of C in the high DOC
87 aquatic system.

88 H3: Rainfall events in the high DOC system will replenish the supply of photolabile material.

89 **2. Methods**

90 **2.1 Study sites**

91 Water samples for the irradiation experiments were collected from two aquatic systems located in
92 peatland catchments. The Black Burn (55°47'34" N; 3°14'35" W; 254 m a.s.l.) is a small headwater
93 stream draining Auchencorth Moss, an ombrotrophic peatland located in central Scotland covering
94 3.35 km² (Billett et al., 2010). The stream is fed by a number of small tributaries from the surrounding
95 peatland, part of which is used for peat extraction. Low density sheep grazing is the primary land use
96 within the catchment and vegetation comprises a *Sphagnum* base layer and hummocks of
97 *Deschampsia flexuosa* and *Eriophorum vaginatum*, or *Juncus effusus*. In the upper catchment shrubs
98 are present, including *Calluna vulgaris*, *Erica tetralix* and *Vaccinium myrtillus* (Dinsmore et al. 2010;
99 Drewer et al., 2010).

100 The Black Burn stream hydrographic record is characterised by a steady base flow and rapid ('flashy')
101 response to rainfall events which typically produce high flow accompanied by elevated DOC
102 concentrations. Annual mean stream water DOC concentrations determined by weekly sampling over
103 a 2 year period were high, at 28.4 ± 1.07 mg L⁻¹ (Dinsmore et al. 2013), with a marked seasonal



104 pattern, characterised by low DOC in winter and high concentrations in summer. In this study, water
105 samples were collected from an established sampling site where DOC concentrations have been
106 recorded for >9 years as part of the Centre for Ecology & Hydrology (CEH) Carbon Catchments
107 project (<https://www.ceh.ac.uk/our-science/projects/ceh-carbon-catchments>).

108 The other sampling site was Loch Katrine (56°25'25" N; 4°45'48" W; 118 m a.s.l.) in the Loch
109 Lomond and Trossachs National Park, Scotland. Loch Katrine has a surface area of 8.9 km² and is fed
110 by ~88 tributaries which predominantly drain a catchment of upland blanket bog (SNH, 2005). Loch
111 water DOC concentrations have been recorded by the Scottish Environment Protection Agency
112 (SEPA) at Ruinn Dubh Aird, a peninsula located at the south eastern end of the loch, which was also
113 selected as the sampling point for this study. DOC concentrations measured approximately six times a
114 year from 2009–2014 were low at 3.68 ± 0.56 mg L⁻¹ (SEPA, personal communication).

115 **2.2 Sample collection**

116 Water was sampled monthly from both sites from May 2014 to May 2015 inclusive (13 samples over
117 the study duration) to characterise seasonal variation in DOC concentration and composition. Samples
118 were collected at 20 cm below the surface of the water in a screw top sterile clear glass bottle. Upon
119 return to the laboratory, samples were stored in the dark at 4°C and exposed to experimental
120 conditions within a week of collection. Additional water sampling to characterise the effect of rainfall
121 events focused on the Black Burn head water system. Intensive stream water sampling was conducted
122 during two rainfall events, one in winter (defined as 1 October to 31 March) and the other during the
123 summer (1 April to 30 September) (Gordon et al., 2004). An automatic water sampler (Teledyne Isco,
124 USA) was programmed to collect a composite 1 L sample of water from the Black Burn into separate
125 polypropylene bottles every 60 minutes (comprising two 500 mL samples collected each 30 minutes)
126 throughout the rainfall events. Stream water sampling in the winter rainfall event was conducted from
127 11:00 on 9 December to 17:00 GMT on 10 December 2014, resulting in 31 samples across the event.
128 Stream water sampling in the summer rainfall event started at 14:30 on 1 September and finished at
129 06:30 GMT on 2 September 2015, resulting in 17 samples. Water samples were transferred into glass



130 bottles from the automatic water sampler for transport to the laboratory and irradiated within 5 days of
131 collection.

132 Throughout the year of sampling, the Black Burn water depth was measured at 15 minute intervals
133 approximately 2 km downstream from the sampling site using a Level Troll pressure transducer (In
134 Situ Inc., USA) with atmospheric correction from a BaroTroll sensor (In situ Inc., USA) located
135 above the water surface. Water depth readings from the pressure transducer were converted to
136 discharge at the sampling site using rating curves ($R^2 > 0.90$) based on flows measured by dilution
137 gauging (Dinsmore et al., 2013). Equivalent hydrological data were not available for Loch Katrine.

138 **2.3 Sample preparation**

139 Prior to experiments water samples were degassed under a vacuum pressure system for 20 minutes to
140 remove dissolved gas from the water and then filtered using syringe driven pore size filters 0.22 μm
141 (Merck Millipore, UK) to exclude microbial activity. 15 mL of filtered sample was immediately
142 transferred into 21 mL quartz vials (Robson Scientific, UK) which were sealed with aluminium crimp
143 tops and rubber butyl plugs (Speck and Burke, UK). All samples were prepared at room temperature
144 in oxygenated conditions.

145 **2.4 Irradiation experiments**

146 Irradiation experiments were conducted using UV-B 313 lamps (Q-Panel Com, USA) covered with
147 125 μm cellulose diacetate (A. Warne, UK) to exclude UV-C (<280 nm) and providing both UV-A
148 (400-315 nm) and UV-B (315-280 nm) exposure. Lamps were mounted inside quartz tubing (Robson
149 Scientific, UK) beneath the water surface in a water bath maintained at 16°C and vials were irradiated
150 sideways while submerged. UV irradiance of the samples was modulated to remain constant
151 throughout the 8-h exposure by measurement with a broad-band sensor (Model PMA2102; Solar
152 Light Inc., USA) held beneath the water surface behind a quartz window of the same thickness as the
153 vials. The sensor was calibrated with a double monochromator scanning spectroradiometer
154 (Irradian™, UK), itself calibrated against a secondary deuterium lamp standard (FEL Lamp, F-1297)
155 operated by the NERC Field Spectroscopy Facility, Edinburgh (<http://fsf.nerc.ac.uk/>). Total



156 unweighted irradiance was 1.81 W m^{-2} in the UV-B, 4.63 W m^{-2} in the UV-A, and photosynthetically
157 active radiation (PAR) was 0.92 W m^{-2} (Supplementary Information Figure S1). These conditions
158 reflect a UV-B irradiance that could be expected on a cloudless summer day in the UK and a
159 significant underestimation of summer time ambient UV-A and PAR radiation. The time duration of
160 the experiment (8 h) was selected to represent a conservative estimate of the exposure time of surface
161 water during transit through a headwater peatland catchment to a marine outlet. Water temperatures of
162 $\sim 16^\circ\text{C}$ were measured in both field sites in May 2014 prior to commencement of the year-long
163 sampling programme and was employed in the experiments to represent summer time conditions.
164 Controls comprising quartz vials containing water samples and wrapped in aluminium foil to exclude
165 radiation were kept in the water bath for the experiment duration, with four replicates of each of the
166 UV-exposed and control samples.

167 To select water samples from the Black Burn for irradiation experiments, POC concentrations, a_{254}
168 values and E4:E6 ratios were measured within 24 h in all samples (using the methods described
169 below) and, from these results, eight stream water samples were selected from each rainfall event
170 which represented the minimum, maximum and median values of these parameters (Supplementary
171 Information Table S1).

172 **2.5 Analytical methods**

173 On each monthly sampling occasion the water dissolved oxygen (DO), conductivity, pH and
174 temperature were measured on site with a handheld Hach HQd multimeter (Hach, USA). Measured
175 volumes of water samples were filtered within 24 h of collection through pre-ashed (8 h at 450°C),
176 pre-weighed Whatman GF/F ($0.7 \mu\text{m}$ pore size) filter papers. POC was determined using loss-on-
177 ignition, following the method of Ball (1964).

178 Following irradiation, partitioning of dissolved C gases from the liquid into the vial headspace was
179 encouraged through use of a wrist action shaker for 30 seconds. CO_2 , CH_4 and CO concentrations
180 were measured in the vial headspace within 8 h of irradiation, using an Agilent gas chromatography
181 (GC) system (Agilent Technologies, USA) equipped with an autosampler and a flame ionisation



182 detector (FID) held at 250°C. The carrier gas was N₂ at a constant flow rate of 45 mL min⁻¹. A
183 methaniser fitted between the column and FID made possible CO₂ and CO measurements. Standard
184 gas mixtures (British Oxygen Company (BOC) Ltd., UK) were used for detector calibration prior to
185 sample analysis (detection limits were: CO₂ 78 ppm, CO 1.6 ppm, CH₄ 0.8 ppm).

186 DOC and dissolved inorganic carbon (DIC) concentrations were measured using a PPM LABTOC
187 Analyser (Pollution and Process Monitoring Ltd., UK) in UV treatment and control samples after
188 exposure. DIC was calculated as the difference between total carbon (TC) and DOC. UV-visible
189 absorbance of UV treatment and control samples contained in a 3.5 mL cuvette was measured at room
190 temperature between 200 and 800 nm at increments of 1 nm using a Jenway spectrophotometer
191 (Model 7315; Bibby Scientific, UK). Deionised water controls were used between each sample.
192 Absorption coefficients a_{λ} were calculated as:

$$193 \quad a_{\lambda} = 2.303 \times \left(\frac{A_{\lambda}}{L} \right) \quad (1)$$

194 where A is the absorbance at each wavelength and L is the path length (m) of the cuvette (Green and
195 Blough, 1994). Specific UV absorbance (SUVA₂₅₄) values, a measure of DOC aromaticity, were
196 determined by dividing the UV absorbance measured at $\lambda = 254$ nm by the DOC concentration
197 (Weishaar et al., 2003). E4:E6 ratios were estimated using the absorbance values at 465 and 665 nm,
198 respectively (Peacock et al., 2014).

199 Fluorescence intensity in water samples filtered to 0.2 μ m was measured using a FluroMax-4
200 spectrofluorometer (Horiba Jobin Yvon Ltd., Japan). The instrument was programmed to scan across
201 excitation wavelengths 200-400 nm (5 nm increments) and emission wavelengths 250-500 nm (2 nm
202 increments) with a 1 nm path interval. Data were obtained at room temperature and were blank
203 corrected using deionised water. Intensity ratios derived using these data allow discrimination
204 between different sources of DOC. Here, the fluorescence index (FI), f_{450}/f_{500} , the ratio of fluorescence
205 intensity at the emission wavelength 450 nm to that at 500 nm at excitation wavelength 370 nm, was
206 calculated to help identify dissolved organic matter (DOM) source material. Values around 1.8



207 suggest autochthonous organic material, whereas values around 1.2 indicate terrestrially derived
208 material (Cory and McKnight, 2005).

209 Lignin phenol concentrations in unirradiated Black Burn water samples were measured using the CuO
210 oxidation method (Benner et al., 2005; Spencer et al., 2008). After filtration to 0.2 μm , 45 mL of
211 water sample was freeze dried to produce lyophilised DOM which was transferred to stainless steel
212 pressure bombs with 1 g of CuO and 100 mg of $\text{Fe}(\text{NH}_4)_2(\text{SO}_4)_2\text{H}_2\text{O}$. Under anaerobic conditions, 8
213 mL of NaOH was added to the bombs before they were sealed. Samples were then oxidised at 155°C
214 for 3 h. Following oxidation, samples were acidified to pH 1 with H_2SO_4 , extracted with ethyl acetate
215 three times, and then passed through Na_2SO_4 drying columns. Samples were dried using a flow of N_2
216 and kept frozen prior to GC analysis. After redissolution in ~200 μL pyridine, lignin phenols were
217 derivatised with bis-trimethylsilyltri-fluoromethylacetamide (BSTFA) and quantified on a GC
218 (Agilent 5890 MkII with twin FID).

219 Eleven lignin phenols were measured, including three p-hydroxybenzene phenols (P): p-
220 hydroxybenzaldehyde, p hydroxyacetophenone, p-hydroxybenzoic acid; three vanillyl phenols (V):
221 vanillin, acetovanillone, vanillic acid; three syringyl phenols (S): syringaldehyde, acetosyringone,
222 syringic acid; and two cinnamyl phenols (C): p-coumaric acid and ferulic acid. Blank controls, taken
223 through the method from CuO oxidation onwards, were quantified and subtracted from sample
224 concentrations. Quantification was achieved through use of cinnamic acid as an internal standard. In
225 addition to total concentration of lignin phenols (Σ_{11}) and carbon normalised yields (Λ_{11}), the ratio of
226 syringyl to vanillyl phenols (S/V), the ratio of cinnamyl to vanillyl (C/V) phenols, the ratio of p-
227 hydroxybenzenes to vanillyl phenols (P/V) and the ratio of acids to aldehydes ($\text{Ad}/\text{Al}_{\text{v,s}}$) were
228 calculated to aid interpretation of the data. Lignin phenols for Loch Katrine samples were not
229 measured due to insufficient production of lyophilised material using the stated method.

230 **2.6 Data analysis**

231 Data collected in the irradiation experiments were tested for normality using the Shapiro-Wilks test
232 and were found to be normally distributed. Unpaired t-tests were conducted between irradiated and



233 unirradiated samples to assess differences in spectral properties, DOC and DIC concentrations, lignin
234 phenol concentration and gaseous production. Pearson correlation coefficients were used to test the
235 potential role of DOC composition and site conditions in regulating photochemical lability, measured
236 as total DOC loss, production of DIC and C gases (CO and CO₂) and change to a₂₅₄ and E4:E6 ratios.

237 Carbon species DOC, DIC, CO₂ and CO measured each month at the Black Burn and Loch Katrine
238 were included in C mass budgets calculated for irradiated and unirradiated samples. By converting all
239 data to mg L⁻¹, the difference in C budget between treatment and control samples could be determined
240 (see Supplementary Information Table S2 for example calculations). To obtain a standard error value
241 for differences between irradiated and control samples, the mean control value was determined and
242 subtracted from each of the irradiated replicates.

243 Correlation coefficients were also calculated between intrinsic sample photoreactivity, measured as
244 total change to C species upon irradiation normalised for initial DOC concentration, and lignin phenol
245 data. The Durbin-Watson statistic was used to test for the presence of autocorrelation in residuals of
246 lignin phenol analyses of stream water samples collected during rainfall events and showed no
247 correlation between the samples. Minitab v.16 (Minitab Inc., USA) was used for all statistical
248 analyses.

249 **3. Results**

250 **3.1 Climate and water chemistry conditions at time of sampling**

251 Total rainfall measured at the European Monitoring and Evaluation Programme (EMEP) supersite at
252 Auchencorth Moss (Torseth et al., 2012) for the 13 month sampling period was 1015 mm. It varied
253 from lowest monthly values in September and April to the highest in October (Figure 1a). The mean
254 air temperature of the study period was 7.7°C, similar to the 8 year average of 7.6°C, and reached a
255 maximum of 27.6°C in July 2014 and a minimum of -7.9°C in January 2015.

256 At Comer meteorological station, located 10 km from the Loch Katrine sampling site, rainfall was
257 considerably higher, totalling 2368 mm over the sampling period (Figure 1b) (Met Office, 2012).



258 Seasonal variation in rainfall was clear, with >40 % of rainfall falling from December to February.
259 Air temperatures were higher than at the Black Burn, with a mean of 10.2°C.

260 Water chemistry differed considerably between the two aquatic systems over the year-long sampling
261 (Table 1). The water temperatures reflected the difference in air temperature between the sites, with
262 higher mean values at Loch Katrine than at the Black Burn. Mean pH at the Black Burn was 5.4,
263 compared to 6.7 at Loch Katrine. Conductivity was more variable at the Black Burn and was on
264 average 53 $\mu\text{S cm}^{-1}$ higher than at Loch Katrine, although values at both sites were low. POC
265 concentrations at the Black Burn were over double those at Loch Katrine. FI values were slightly
266 higher at the Black Burn, but at both sites were low and stable, indicative of terrestrially derived DOC
267 material (Cory and McKnight, 2005)

268 DOC concentrations at the Black Burn ranged from 14.2 to 50.9 mg L^{-1} (Figure 2) and showed a
269 similar seasonal pattern as described in Dinsmore et al. (2013). Concentrations were lowest in late
270 winter and highest in autumn; the latter consistent with increased organic matter inputs to the stream
271 from flushing of soils during autumn rainfall events.

272 At Loch Katrine, DOC concentrations were low and consistent, ranging from 3.10 to 5.82 mg L^{-1} .
273 Concentrations were lowest in spring and highest in summer. SUVA_{254} values at the Black Burn were
274 higher than at Loch Katrine, suggesting that the DOC pool was comprised of a greater percentage of
275 aromatic material (Weishaar et al., 2003). The E4:E6 ratio at the Black Burn varied considerably over
276 the sampling period, ranging from 1.0 to 10.2. At Loch Katrine, the E4:E6 ratios were lower and less
277 variable, but are a less meaningful parameter in the low DOC concentration Loch Katrine samples due
278 to minimal absorbance in wavelengths greater than 400 nm.

279 **3.2 Optical changes in water samples upon irradiation**

280 Absorbance coefficients typically decreased upon irradiation of water samples, with the strongest
281 decrease occurring in the UV part of the spectrum at ~225 nm, and a smaller inflection at ~300 nm
282 (Figure 3). The maximum change in absorbance upon irradiation was a factor of 4 higher in water
283 samples from the Black Burn than from Loch Katrine. In the Black Burn, decreases in absorbance



284 were greater in the summer and autumn, whereas at Loch Katrine the decreases in absorbance were
285 greater in the winter and spring.

286 Positive values (where dark control samples showed a greater drop in absorbance upon irradiation
287 than light exposed samples) were recorded for summer water samples from Loch Katrine. E4:E6
288 ratios decreased by a mean of 1.52 in irradiated Black Burn water samples, indicating accumulation of
289 increasingly humic material in the remaining DOC pool during light exposure. At Loch Katrine,
290 E4:E6 ratios decreased by a mean of 0.21 upon irradiation.

291 3.3 Carbon budget changes upon irradiation

292 Typically, DOC concentrations in Black Burn water samples decreased after light exposure compared
293 to unirradiated controls (Figure 4a). Mean change in DOC in irradiated samples from the Black Burn
294 for the whole sampling period was $-2.14 \text{ mg C L}^{-1}$ (ranging from 0.06 to $-4.35 \text{ mg C L}^{-1}$ for individual
295 months). DOC decreased after irradiation in all Black Burn samples with the exception of September
296 2014, indicating a photolabile DOC pool for most of the year. In contrast, in water samples from Loch
297 Katrine irradiation induced DOC losses occurred in 6 of 13 samples and small gains were observed in
298 7 of 13 samples (Figure 4b). Whilst these results should be interpreted with caution as small
299 differences in DOC concentrations ($<0.5 \text{ mg C L}^{-1}$) are below the instrument detection limit, they
300 suggest that the DOC pool in Loch Katrine was largely recalcitrant to photochemical degradation.

301 Irradiation resulted in notable photoproduction of DIC, CO_2 and CO from Black Burn samples. DIC
302 concentration increased by a mean of 0.77 mg C L^{-1} for the whole sampling period, although
303 production across the samples was highly variable between months. CO_2 was the most abundant
304 photoproduct and was produced at a mean rate of 1.2 mg C L^{-1} across all monthly samples. At Loch
305 Katrine, CO_2 production was two orders of magnitude lower than in the Black Burn, produced at a
306 mean rate of 0.06 mg C L^{-1} . In all monthly water samples from both sites CO concentrations increased
307 in the irradiation experiments, with mean production rates of 0.07 and 0.01 mg C L^{-1} observed for
308 Black Burn and Loch Katrine samples, respectively.



309 Carbon mass budgets for DOC loss and photoproduct accumulation (DIC, CO₂ and CO) in water
310 samples were calculated for all the irradiation experiments. Budgets for all monthly water samples
311 from the Black Burn were balanced to within $\pm 5.1\%$ of the total measured C concentration. For Loch
312 Katrine water samples, budgets were balanced to within $\pm 11\%$. The lower accuracy of budget closure
313 in the Loch Katrine samples is likely due to lower overall C concentrations, which are more
314 susceptible to measurement error. CH₄ was detected in all samples at very low levels, with mean
315 concentrations of 0.63 and 0.57 $\mu\text{g L}^{-1}$ detected at the Black Burn and Loch Katrine, respectively, and
316 thus were not included in the mass calculations.

317 Intrinsic photoreactivity of C in the Black Burn ranged from 0.02 to 0.15 mg C/mg DOC L⁻¹ and was
318 highest in August (Figure 4a). Photoreactivity peaked again in November and remained elevated until
319 January. Lowest sample photoreactivity was detected in September. At Loch Katrine, mean C
320 photoreactivity was 0.004 mg C/mg DOC L⁻¹, with a maximum of 0.09 mg C/mg DOC L⁻¹ detected in
321 July.

322 **3.4 Factors influencing carbon budget changes**

323 Factors influencing irradiation induced changes to C species and spectral properties in Black Burn
324 water samples were investigated using Pearson correlations (Table 2). Loss of DOC, absorbance at
325 254 nm and production of both CO₂ and CO were significantly positively correlated with initial DOC
326 concentration. Initial E4:E6 ratios had positive coefficient values with all light induced changes to the
327 DOM pool, whilst FI values were all negative, although most of these correlations were not
328 significant.

329 Of the meteorological and discharge variables investigated, air temperature and PAR were
330 significantly negatively correlated with changes to E4:E6 ratios. Total monthly rainfall had positive
331 coefficient values with irradiation induced changes to the DOM pool. Correlations between C species
332 changes and discharge were less consistent, although mean monthly discharge was significantly
333 positively correlated with changes to E4:E6 ratios.



334 **3.5 Effect of rainfall events on carbon photo-processing in Black Burn water samples**

335 The Black Burn was sampled hourly during a winter rainfall event, with collection commencing 6 h
336 before peak rainfall (Figure 5a). Total rainfall during the event, which we define here as the water
337 sampling period, was 19.6 mm, with an hourly maximum of 3.3 mm and rainfall recorded in 22 of the
338 31 sampling hours. Stream discharge peaked at 391 L s⁻¹ although a separate smaller peak of 266 L s⁻¹
339 also occurred during the sampling period.

340 During the event, an initial dilution of stream DOC concentrations was followed by recovery to pre-
341 event levels (Figure 5a). DOC was most photoreactive at 06:00, with DOC concentration reduced
342 after irradiation by 6.72 mg L⁻¹. DOC loss in this sample was greater than at any time through the
343 year-long study (Figure 4a), even though the DOC concentration (44.4 mg L⁻¹) was within the range
344 of measured monthly concentrations. The greatest irradiation induced increase in CO₂ concentration
345 (2.25 mg L⁻¹) occurred in the first event sample at 11:00, collected prior to rainfall input.
346 Photoreactivity was lowest at 12:00, and was similarly low in the sample collected at 17:00, which
347 coincided with peak rainfall.

348 In the late summer rainfall event occurring at the end of an extended period of base flow in the Black
349 Burn (Supplementary Information Figure S2), 3.2 mm of rainfall was recorded with a maximum
350 hourly total of 2.2 mm. Samples were collected from 14:30 to 06:30, with rainfall only occurring
351 between 16:30 and 18:30. Discharge remained low and relatively stable throughout the event, with a
352 mean flow of 6.14 L s⁻¹. Rainfall marginally diluted the stream DOC concentrations (Figure 5b).
353 Photo-induced changes were much smaller than in the winter event and maximum DOC losses were a
354 factor of 2.5 lower than the mean DOC reduction observed in the Black Burn monthly water sample
355 experiments (Figure 4a). Photoreactivity was lowest in the initial sample collected at 14:30 prior to
356 rainfall and coinciding with the highest discharge during the sampling period. Photoreactivity was
357 highest in the 19:30 sample collected 3 h after peak rainfall.



358 3.6 Lignin phenol composition of Black Burn water samples

359 To understand the effect of DOM composition on photolability, lignin phenols were measured in all
360 the Black Burn monthly and rainfall events water samples prior to the irradiation experiments.

361 Dissolved lignin concentrations ranged from 15.3 to 108 $\mu\text{g L}^{-1}$ (mean = 52.8; n = 28) and were
362 significantly positively correlated with sample DOC concentration (Pearson = 0.831; $p < 0.01$)
363 (Supplementary Information Figure S3). Carbon normalised yields were between 0.71 and 2.66 mg
364 (100 mg OC) $^{-1}$. The contribution of individual phenol groups to the lignin signature varied between
365 monthly samples of the year-long study and the rainfall events (Figure 6). In the monthly samples, the
366 P phenols were most abundant, followed by V phenols (Figure 6a). Samples in the winter rainfall
367 event contained higher and more variable mean yields for each phenol group, with S phenols most
368 abundant, followed by V phenols and P phenols.

369 Overall yields were significantly lower (1-way ANOVA, $p < 0.01$) during the summer rainfall event.
370 As in the year-long samples, P phenols were the most abundant, followed by S phenols and V
371 phenols. Across all three sampling regimes, the contribution of C phenols to the overall lignin
372 signature was smallest.

373 P:V ratios, an indication of *Sphagnum* derived DOC (see section 4.2), ranged from 0.83 to 1.69 across
374 all samples, indicating significant temporal variability in DOM source material. Photoreactivity was
375 significantly negatively correlated with P:V ratios when all samples were combined in a correlation
376 analysis (-0.523; $p < 0.01$) (Figure 7a). This suggests that the relative abundance of P versus V
377 phenols contributed considerably to sample photoreactivity. The lowest P:V ratios were in winter
378 rainfall event samples, where photoreactivity was highest.

379 Ad:Al_{v,s} ratios, which are an indicator of sample degradation, ranged from 0.58 to 1.26, towards the
380 lower end of reported values in the literature (Winterfeld et al., 2015). Photoreactivity was also
381 significantly negatively correlated with Ad:Al ratios (-0.492; $p < 0.01$) (Figure 7b) and again lower
382 ratios typically occurred in winter rainfall event samples.



383 4. Discussion

384 4.1 Peatlands as a source of photochemically labile DOC

385 Photo-processing resulted in considerable DOC loss from water samples from the Black Burn. Mean
386 DOC loss in the 8 h irradiation experiments conducted on the monthly water samples was 6% relative
387 to initial concentrations. Percentage DOC losses determined here are similar to those reported from
388 irradiation experiments conducted over similar timescales using stream water draining a boreal
389 watershed (3–10 % DOC loss over 10 h; Franke et al., 2012 and 11% TOC loss over 19 h; Köhler et
390 al., 2002). Photochemical transformations were low in the Loch Katrine samples, with minimal losses
391 to the DOC pool (-0.03%; mean from year-long study). Whilst our sites were not located within the
392 same watershed, it seems likely that position within the catchment plays a role in determining the
393 photolability of DOC. The Black Burn headwater stream at Auchencorth Moss receives fresh inputs
394 of DOC from the surrounding peatland catchment and material has less time for light exposure in the
395 water column relative to the DOC in the reservoir system. DOC losses may occur in Loch Katrine
396 soon after water entry into the loch but, due to long water residence times, DOC may have become
397 recalcitrant to photo-processing by the time of sample collection. Catalán et al. (2016) observed a
398 negative relationship between organic carbon decay and water retention time, resulting in decreased
399 organic carbon reactivity along the continuum of inland waters. $SUVA_{254}$ data suggest that DOC in
400 Loch Katrine samples was less aromatic than in the Black Burn (Table 1), with values indicating an
401 approximate humic content of 30% based on the findings of Weishaar et al. (2003). As humic
402 molecules are more labile to photo-processing, irradiation had a greater effect on the stream samples
403 relative to the reservoir samples.

404 Strong seasonal fluctuations in DOC concentration and composition occurred in the Black Burn, in
405 agreement with patterns observed in the same system by Dinsmore et al. (2013). DOC concentrations
406 were highest in the late autumn, consistent with a flushing effect whereby soil organic material
407 produced over the summer is mobilised and delivered to aquatic environments by more intense
408 rainfall after a prolonged, relatively dry period (Fenner et al., 2005). Positive correlation between the
409 irradiation induced change in the E4:E6 ratio and mean monthly discharge suggest that hydrological



410 conditions in the month prior to sampling significantly influence the reactivity of the sample, with
411 high flow delivering more reactive carbon to the stream. Overall the magnitude of photo-induced C
412 losses was significantly positively correlated with DOC concentration in the year-long Black Burn
413 dataset. However, despite low DOC concentrations, photoreactivity remained elevated in January.
414 This suggests that even when lower DOC concentrations are detected in aquatic systems, the DOC
415 may be intrinsically more photoreactive due to its aromatic content and minimal light exposure
416 history.

417 Lowest DOC concentrations were observed in the late winter and early spring, due to depletion of soil
418 organic C within the catchment by autumn and winter rainfall events. Low rainfall inputs limit the
419 recharge of fresh, photolabile material to the stream and may account for the reduction in DOC
420 photoreactivity detected in September. Furthermore, due to longer residence time in the water column,
421 these samples may have already been degraded by natural light. A previous study at the Black Burn
422 reported ^{13}C enrichment of stream water DOC in September, consistent with increased in-stream
423 processing at this time of year (Leith et al., 2014). Reductions in intrinsic DOC photolability during
424 summer have similarly been reported in northern lakes (Vachon et al., 2016) and a boreal watershed
425 (Franke et al., 2012). Another minimum in photoreactivity occurred in April, where SUVA_{254} data
426 indicate decreased contribution of aromatic material to C within the stream. Although algal abundance
427 was not measured during this study, production of DOC from such sources would account for the
428 reduction in photolability (Nyugen et al., 2005).

429 Whilst DOC losses from Loch Katrine water samples were minimal, the peak in photolability,
430 indicated by the greatest absorbance reduction in the light exposure experiments, occurred in spring.
431 Similar seasonal photolability peaks have been observed in northern lakes (Vachon et al., 2016) and
432 boreal streams (Porcal et al., 2013) and are partly attributed to mobilisation of terrigenous material
433 with high flows associated with spring snow melt. The magnitude of melt in the Loch Katrine
434 catchment will be considerably less than in snow dominated northern catchments (e.g. Laudon et al.,
435 2013), although increased flow and stream water chemistry changes with spring snow melt have been
436 reported in upland Scottish catchments (Abrahams et al., 1989; Gilvear et al., 2002).



437 Absorbance increased in light exposed samples during irradiation in summer Loch Katrine samples,
438 indicating production of DOC. Prior filtration of samples to 0.22 μm means that this effect is unlikely
439 to be the result of microbial DOC production. A possible explanation for increased absorbance in the
440 irradiated water samples is the formation of an iron (Fe)-DOC complex, since the reaction kinetics of
441 Fe-DOC complexes are directly affected by light exposure (Maranger and Pullin, 2003). Whilst Fe
442 concentrations were not measured in this study, in a long term SEPA bimonthly measurement
443 campaign (2009-2013) at Loch Katrine, peak Fe concentrations in August of up to 0.50 mg L^{-1} were
444 detected, corresponding to the time of year when we found increased absorbance in water samples. As
445 the data set does not cover the sampling period, the role of Fe-DOC complexes in producing the
446 observed effect cannot be directly determined; however the role of micronutrients in peatland aquatic
447 C cycling should be further investigated.

448 **4.2 Importance of rainfall events in mobilising photolabile material**

449 Dissolved lignin phenol composition indicates that different sources of plant material were mobilised
450 as a result of rainfall in the Auchencorth Moss catchment. High P:V ratios have been used as an
451 indicator of peatland inputs to aquatic systems, as *Sphagnum* acid typical of peatlands is converted
452 into P phenols during lignin extraction (Fichot et al., 2016; Winterfeld et al., 2015). Typically P
453 phenols constituted the largest contribution to the total lignin concentration of the measured phenols,
454 consistent with *Sphagnum* inputs. However, during the winter rainfall event where stream discharge
455 was considerably higher than the year-long mean value, the largest contribution to total lignin
456 concentration was from S and V phenols (Figure 6). The former are reported to be the most
457 photolabile phenol (Opsahl and Benner, 1998) and are unique to woody angiosperms. This suggests
458 that hydrological pathways within the catchment were activated upon rainfall, causing DOC release
459 from soil profiles associated with angiosperm plant material. Potential sources within the Auchencorth
460 upper catchment are *Calluna vulgaris*, *Erica tetralix* and *Vaccinium myrtillus*. Further evidence of the
461 operation of variable source areas in the catchment was the observation of delayed input of water,
462 containing high CO_2 concentrations, from the deep peat area in the upper catchment at Auchencorth
463 Moss during a storm event (Dinsmore and Billett, 2008). Low P:V values and high lignin



464 concentrations have been reported during peak flow in Arctic rivers, and the reverse during base flow
465 (Amon et al., 2012). As samples with low P:V values were typically more photoreactive (Figure 7a),
466 our data indicate that rainfall events are important in mobilising photolabile material from this
467 catchment.

468 Elevated Ad:Al_{v,s} ratios have previously been interpreted as indicators of decomposition of organic
469 matter resulting from preferential degradation of aldehydes relative to acids (Spencer et al., 2009). In
470 the Black Burn water samples, lowest ratios were measured in the winter rainfall event. This implies
471 that DOC mobilised during rainfall is less degraded relative to base flow DOC, in agreement with
472 previous studies of peatland high flow events which detected increased contribution of near surface
473 flow and younger DOC (Clark et al., 2008). The form of the degradation, either microbial or
474 photochemical, cannot be distinguished using these data. However, based on the higher measured
475 photoreactivity of samples with lower ratios (Figure 7b), light exposure history may be one of the key
476 moderators of Ad:Al_{v,s} ratios in the Black Burn. High flow events release fresh DOC from soils
477 derived from recent plant material (Evans et al., 2007) and may have significant implications for C
478 processing rates in streams as they are recharged with labile material (Lapierre et al., 2013).

479 Whilst the samples collected during the winter rainfall event were clearly distinct in composition
480 relative to samples from the year-long study, the summer rainfall event samples had similar P:V and
481 Ad:Al_{v,s} ratios, but significantly lower photoreactivity and overall lignin yields (Figures 5b, 6c, 7).
482 This could be attributed to the timing of sample collection in early September at the end of summer,
483 where considerable degradation may have already occurred across all phenol groups so that the DOC
484 pool remaining was more recalcitrant to further photo-processing. Discharge data indicate that there
485 was no discernible flushing effect during the summer rainfall event, with slight decreases in DOC
486 concentration attributed to dilution of the stream water by direct rainfall inputs or overland flow. The
487 abundance of P phenols within the samples suggest that passive transfer of DOC from the riparian
488 zone, which is dominated by *Sphagnum* and *Juncus* vegetation, to the stream was the dominant mode
489 of stream DOC recharge at this time of year (Jeanneau et al., 2015). The summer rainfall event



490 samples were notably depleted in V phenols, suggesting that these phenols exert an important control
491 on sample photoreactivity in addition to S phenols.

492 **4.3 Implications for photochemical turnover of DOC in aquatic systems**

493 DOC loss from samples upon irradiation resulted in significant production of CO₂. The mass budget
494 calculations for Black Burn water samples show that a mean of ~46% of DOC loss in the irradiation
495 experiments was accounted for by production of CO₂. Dinsmore et al. (2010) estimate that 108 ± 62.7
496 kg DOC yr⁻¹ is exported to the Black Burn from the Auchencorth Moss catchment. Based on our
497 finding that 7% of DOC is removed via photo-processing, and assuming that 46% of this loss is
498 converted to CO₂ and also that UV-B irradiance was comparable to a clear sky summer day, we
499 estimate a potential evasion loss of 3.48 ± 2.02 kg CO₂ yr⁻¹ to the atmosphere. Whilst this calculation
500 makes significant assumptions in upscaling from 8 h exposure experiments, it highlights the potential
501 importance of photo-processing in the turnover of aquatic C and the need for more in situ studies.

502 Due to the effects of bank shading and short transit time of water within the immediate catchment,
503 light driven instream DOC processing is unlikely to be significant. The river continuum concept
504 suggests that increased DOC processing will occur further downstream, where the channel widens
505 (Vannote et al., 1980), and will be partly controlled by the stream water mean transit time (McDonnell
506 et al., 2010; McGuire and McDonnell, 2006). Based on mean velocity (~ 0.58 m s⁻¹) of a larger nearby
507 river (Ledger, 1981), we estimate a mean water transit time of 19 h from the Black Burn at
508 Auchencorth Moss to its coastal outlet in the River Esk 34 km downstream, considerably longer than
509 the exposure time in our experiments. However, in a study of 1st to 4th order streams in Sweden no
510 significant change to DOM composition as stream order increased was detected and this was partly
511 attributed to short transit times (<2 days) restricting DOC processing (Kothawala et al. 2015).
512 Peatland derived carbon in this study is clearly photoreactive, but limited time for in-stream
513 processing may render photo-processing unimportant in freshwater aquatic C budgets.

514 Determining the C cycling implications of this study is further complicated as the most photoreactive
515 material was recorded during a heavy winter rainfall event. The potential for photochemical



516 transformation of DOC within the freshwater aquatic environment would have been limited due to
517 low light availability, extensive cloud cover and increased stream water transit times associated with
518 the event. During the year-long study period, 12 rainfall events occurred which resulted in similar
519 flow conditions in the Black Burn (stream discharge exceeding 250 L s^{-1}), with a maximum discharge
520 of 2059 L s^{-1} in a late winter storm. Of these high flow events, 11 occurred during winter and one in
521 summer and hence, whilst large quantities of photoreactive material may have been mobilised during
522 heavy rainfall, the likelihood of in-stream processing would remain small. Increases in precipitation,
523 with more frequent and intense rainfall events, are expected with climate change (Capell et al., 2013;
524 Edenhofer et al., 2014) with heavier summer downpours predicted in the UK (Kendon et al., 2014).
525 Thus, although the contribution of rainfall events to freshwater aquatic C cycling in this study is likely
526 to be minimal, they could become more significant if heavy rainfall events occur more frequently in
527 summer.

528 **Author Contributions**

529 AEP collected field samples and undertook laboratory analyses. Data analysis and writing of the paper
530 were also carried out by AEP. KVH, ARM and KJD provided guidance on the scope and design of the
531 project, and contributed to the editing of the manuscript.

532 **Acknowledgements**

533 This work was funded by a Natural Environment Research Council (NERC) PhD studentship
534 (NE/K500835/1). Further support was provided by a Moss PhD scholarship courtesy of Derek and
535 Maureen Moss. The Irradian™ spectroradiometer used in this study was calibrated by Chris McLellan
536 at the NERC Field Spectroscopy Facility. We thank Stephen Mowbray for his assistance with lignin
537 phenol analyses and Andrew Addison for his contribution to fieldwork. We also thank Tony
538 Dickinson and Jim Donnelly at the University of Central Lancashire for use of a Horiba FluroMax-4
539 spectrofluorometer.

540 **References**



- 541 Abrahams, P. W., Tranter, M., Davies, T. D. and Blackwood, I. L.: Geochemical studies in a remote
542 scottish upland catchment II. Streamwater chemistry during snow-melt, *Water Air Soil Pollut.*, 43(3-
543 4), 231–248, doi:10.1007/BF00279194, 1989.
- 544 Amon, R. M. W., Rinehart, A. J., Duan, S., Louchouart, P., Prokushkin, A., Guggenberger, G.,
545 Bauch, D., Stedmon, C., Raymond, P. A., Holmes, R. M., McClelland, J. W., Peterson, B. J., Walker,
546 S. A. and Zhulidov, A. V.: Dissolved organic matter sources in large Arctic rivers, *Geochim.*
547 *Cosmochim. Acta*, 94, 217–237, doi:10.1016/j.gca.2012.07.015, 2012.
- 548 Austnes, K., Evans, C. D., Eliot-Laize, C., Naden, P. S. and Old, G. H.: Effects of storm events on
549 mobilisation and in-stream processing of dissolved organic matter (DOM) in a Welsh peatland
550 catchment, *Biogeochemistry*, 99(1), 157–173, doi:10.1007/s10533-009-9399-4, 2010.
- 551 Ball, D. F.: Loss-on-ignition as an estimate of organic matter and organic carbon in non-calcareous
552 soils, *J. Soil Sci.*, 15, 84–92, doi:10.1111/j.1365-2389.1964.tb00247.x, 1964.
- 553 Benner, R., Louchouart, P. and Amon, R. M. W.: Terrigenous dissolved organic matter in the Arctic
554 Ocean and its transport to surface and deep waters of the North Atlantic, *Global Biogeochem. Cycles*,
555 19, 1–11, doi:10.1029/2004GB002398, 2005.
- 556 Billett, M. F., Charman, D. J., Clark, J. M., Evans, C. D., Evans, M. G., Ostle, N. J., Worrall, F.,
557 Burden, A., Dinsmore, K. J., Jones, T., McNamara, N. P., Parry, L., Rowson, J. G. and Rose, R.:
558 Carbon balance of UK peatlands: current state of knowledge and future research challenges, *Clim.*
559 *Res.*, 45, 13–29, doi:10.3354/cr00903, 2010.
- 560 Capell, R., Tetzlaff, D. and Soulsby, C.: Will catchment characteristics moderate the projected effects
561 of climate change on flow regimes in the Scottish Highlands?, *Hydrol. Process.*, 27, 687–699, 2013.
- 562 Catalán, N., Marcé, R., Kothawala, D. N., Tranvik, L. J.: Organic carbon decomposition rates
563 controlled by water retention time across inland waters, *Nat. Geosci.*, doi:doi:10.1038/ngeo2720,
564 2016.
- 565 Clark, J. M., Lane, S. N., Chapman, P. J. and Adamson, J. K.: Export of dissolved organic carbon
566 from an upland peatland during storm events: Implications for flux estimates, *J. Hydrol.*, 347(3-4),



- 567 438–447, doi:10.1016/j.jhydrol.2007.09.030, 2007.
- 568 Clark, J. M., Lane, S. N., Chapman, P. J. and Adamson, J. K.: Link between DOC in near surface peat
569 and stream water in an upland catchment, *Sci. Total Environ.*, 404(2-3), 308–315,
570 doi:10.1016/j.scitotenv.2007.11.002, 2008.
- 571 Cory, R. M. and McKnight, D. M.: Fluorescence spectroscopy reveals ubiquitous presence of
572 oxidized and reduced quinones in dissolved organic matter, *Environ. Sci. Technol.*, 39(21), 8142–
573 8149, doi:10.1021/es0506962, 2005.
- 574 Cory, R. M., Ward, C. P., Crump, B. C. and Kling, G. W.: Sunlight controls water column processing
575 of carbon in arctic fresh waters, *Science*, 345(6199), 925–928, doi:10.1126/science.1253119, 2014.
- 576 Dinsmore, K. J. and Billett, M. F.: Continuous measurement and modeling of CO₂ losses from a
577 peatland stream during stormflow events, *Water Resour. Res.*, 44(12), doi:10.1029/2008WR007284,
578 2008.
- 579 Dinsmore, K. J., Billett, M. F., Skiba, U. M., Rees, R. M., Drewer, J. and Helfter, C.: Role of the
580 aquatic pathway in the carbon and greenhouse gas budgets of a peatland catchment, *Glob. Chang.*
581 *Biol.*, 16, 2750–2762, doi:10.1111/j.1365-2486.2009.02119.x, 2010.
- 582 Dinsmore, K. J., Billett, M. F. and Dyson, K. E.: Temperature and precipitation drive temporal
583 variability in aquatic carbon and GHG concentrations and fluxes in a peatland catchment, *Glob.*
584 *Chang. Biol.*, 19, 2133–2148, doi:10.1111/gcb.12209, 2013.
- 585 Drewer, J., Lohila, A., Aurela, M., Laurila, T., Minkkinen, K., Penttilä, T., Dinsmore, K. J.,
586 McKenzie, R. M., Helfter, C., Flechard, C., Sutton, M. A. and Skiba, U. M.: Comparison of
587 greenhouse gas fluxes and nitrogen budgets from an ombrotrophic bog in Scotland and a
588 minerotrophic sedge fen in Finland, *Eur. J. Soil Sci.*, 61(5), 640–650, doi:10.1111/j.1365-
589 2389.2010.01267.x, 2010.
- 590 Edenhofer, O., Pichs-Madruga, R., Sokona, Y., Farahani, E., Kadner, S., Seyboth, K., Adler, A.,
591 Baum, I., Brunner, S., Eickemeier, P., Kriemann, B., Savolainen, J., Schlömer, S., von Stechow, C.,
592 Zwickel, T. and Minx, J. C.: IPCC, 2014: Summary for Policymakers., 2014.



- 593 Fellman, J. B., Hood, E., Edwards, R. T. and D'Amore, D. V.: Changes in the concentration,
594 biodegradability, and fluorescent properties of dissolved organic matter during stormflows in coastal
595 temperate watersheds, *J. Geophys. Res. Biogeosciences*, 114(1), doi:10.1029/2008JG000790, 2009.
- 596 Fichot, C. G., Benner, R., Kaiser, K., Shen, Y., Amon, R. M. W., Ogawa, H., Lu, C.-J.: Predicting
597 Dissolved Lignin Phenol Concentrations in the Coastal Ocean from Chromophoric Dissolved Organic
598 Matter (CDOM) Absorption Coefficients, *Front. Mar. Sci.*, 3:7, 1–16, 2016.
- 599 Franke, D., Hamilton, M. W. and Ziegler, S. E.: Variation in the photochemical lability of dissolved
600 organic matter in a large boreal watershed, *Aquat. Sci.*, 74, 751–768, doi:10.1007/s00027-012-0258-3,
601 2012.
- 602 Gilvear, D. J., Heal, K. V. and Stephen, A.: Hydrology and the ecological quality of Scottish river
603 ecosystems, *Science of the Total Environment*, 294, 131–159., 2002.
- 604 Gordon, N. D., T. A. McMahon, B. L. Finlayson, C. J. Gippel, and R. J. N.: *Stream Hydrology: An*
605 *Introduction for Ecologists*, Wiley., 2004.
- 606 Jeanneau, L., Denis, M., Pierson-Wickmann, A. C., Gruau, G., Lambert, T. and Petitjean, P.: Sources
607 of dissolved organic matter during storm and inter-storm conditions in a lowland headwater
608 catchment: Constraints from high-frequency molecular data, *Biogeosciences*, 12(14), 4333–4343,
609 doi:10.5194/bg-12-4333-2015, 2015.
- 610 Kendon, E., Roberts, N. and Fowler, H.: Heavier summer downpours with climate change revealed by
611 weather forecast resolution model, *Nat. Clim. Chang.*, 4, 1–7, doi:10.1038/NCLIMATE2258, 2014.
- 612 Koehler, B., Landelius, T., Weyhenmeyer, G. a, Machida, N. and Tranvik, L. J.: Sunlight-induced
613 carbon dioxide emissions from inland waters, *Global Biogeochem. Cycles*, 28, 696–711,
614 doi:10.1002/2014GB004850.Received, 2014.
- 615 Kohler, S., Buffam, I., Jonsson, A. and Bishop, K.: Photochemical and microbial processing of stream
616 and soil water dissolved organic matter in a boreal forested catchment in northern Sweden, *Aquat.*
617 *Sci.*, 64(3), 269–281, doi:10.1007/s00027-002-8071-z, 2002.
- 618 Kothawala, D. N., Ji, X., Laudon, H., Ågren, A. M., Futter, M. N., Köhler, S. J. and Tranvik, L. J.:



- 619 The relative influence of land cover, hydrology, and in-stream processing on the composition of
620 dissolved organic matter in boreal streams, *J. Geophys. Res. Biogeosci.*, 120(8), 1491–1505,
621 doi:10.1002/2015JG002946, 2015.
- 622 Lapierre, J.-F., Guillemette, F., Berggren, M. and del Giorgio, P. A.: Increases in terrestrially derived
623 carbon stimulate organic carbon processing and CO₂ emissions in boreal aquatic ecosystems, *Nat.*
624 *Commun.*, 4, 2972, doi:10.1038/ncomms3972, 2013.
- 625 Laudon, H., Tetzlaff, D., Soulsby, C., Carey, S., Seibert, J., Buttle, J., Shanley, J., McDonnell, J. J.
626 and McGuire, K.: Change in winter climate will affect dissolved organic carbon and water fluxes in
627 mid-to-high latitude catchments, *Hydrol. Process.*, 27(5), 700–709, doi:10.1002/hyp.9686, 2013.
- 628 Ledger, D. C.: The velocity of the River Tweed and its tributaries, *Freshw. Biol.*, 11, 1–10, 1981.
- 629 Maranger, R. and Pullin, M. J.: Elemental complexation of dissolved organic matter in lakes:
630 implications for Fe speciation and the bioavailability of Fe and P, in *Aquatic Ecosystems: Interactivity*
631 *of Dissolved Organic Matter*, edited by R. L. Findlay, S.E.G., Sinsabaugh, pp. 186–207, Academic
632 Press, San Diego., 2003.
- 633 McDonnell, J. J., McGuire, K., Aggarwal, P., Beven, K. J., Biondi, D., Destouni, G., Dunn, S., James,
634 A., Kirchner, J., Kraft, P., Lyon, S., Maloszewski, P., Newman, B., Pfister, L., Rinaldo, A., Rodhe,
635 A., Sayama, T., Seibert, J., Solomon, K., Soulsby, C, S.: How old is streamwater? Open questions in
636 catchment transit time conceptualization, modelling and analysis, *Hydrol. Process.*, 24, 1745–1754,
637 doi:doi: 10.1002/hyp.7796, 2010.
- 638 McGuire, K. J. and McDonnell, J. J.: A review and evaluation of catchment transit time modeling, *J.*
639 *Hydrol.*, 330(3-4), 543–563, doi:10.1016/j.jhydrol.2006.04.020, 2006.
- 640 Met Office: Met Office Integrated Data Archive System (MIDAS) Land and Marine Surface Stations
641 Data (1853-current), NCAS Br. Atmos. Data Cent. [online] Available from:
642 <http://catalogue.ceda.ac.uk/uuid/220a65615218d5c9cc9e4785a3234bd0>, 2012.
- 643 Moody, C. S., Worrall, F., Evans, C. D. and Jones, T. G.: The rate of loss of dissolved organic carbon
644 (DOC) through a catchment, *J. Hydrol.*, 492, 139–150, doi:10.1016/j.jhydrol.2013.03.016, 2013.



- 645 Opsahl, S. and Benner, R.: Photochemical reactivity of dissolved lignin in river and ocean waters,
646 *Limnol. Oceanogr.*, 43, 1297–1304, doi:10.4319/lo.1998.43.6.1297, 1998.
- 647 Peacock, M., Evans, C. D., Fenner, N., Freeman, C., Gough, R., Jones, T. G. and Lebron, I.: UV-
648 visible absorbance spectroscopy as a proxy for peatland dissolved organic carbon (DOC) quantity and
649 quality: considerations on wavelength and absorbance degradation, *Environ. Sci. Process. Impacts*,
650 10–12, doi:10.1039/c4em00108g, 2014.
- 651 SNH Report 093: Environmental Resources Management (2005). Loch Lomond and the Trossachs
652 landscape character assessment. Scottish Natural Heritage Commissioned Report No. 093 (ROAME
653 No. BAT/AA302/00/01/123).
- 654 Spencer, R. G. M., Aiken, G. R., Wickland, K. P., Striegl, R. G. and Hernes, P. J.: Seasonal and
655 spatial variability in dissolved organic matter quantity and composition from the Yukon River basin,
656 Alaska, *Global Biogeochem. Cycles*, 22, doi:10.1029/2008GB003231, 2008.
- 657 Spencer, R. G. M., Stubbins, A., Hernes, P. J., Baker, A., Mopper, K., Aufdenkampe, A. K., Dyda, R.
658 Y., Mwamba, V. L., Mangangu, A. M., Wabakanghanzi, J. N. and Six, J.: Photochemical degradation
659 of dissolved organic matter and dissolved lignin phenols from the Congo River, *J. Geophys. Res.*,
660 114, doi:10.1029/2009JG000968, 2009.
- 661 Stubbins, A., Law, C. S., Uher, G. and Upstill-Goddard, R. C.: Carbon monoxide apparent quantum
662 yields and photoproduction in the Tyne estuary, *Biogeosciences*, 8(3), 703–713, doi:10.5194/bg-8-
663 703-2011, 2011.
- 664 Sulzberger, B. and Durisch-Kaiser, E.: Chemical characterization of dissolved organic matter (DOM):
665 A prerequisite for understanding UV-induced changes of DOM absorption properties and
666 bioavailability, *Aquat. Sci.*, 71, 104–126, doi:10.1007/s00027-008-8082-5, 2009.
- 667 Torseth, K., Aas, W., Breivik, K., Fjæraa, A. M., Fiebig, M., Hjellbrekke, A. G., Lund Myhre, C.,
668 Solberg, S. and Yttri, K. E.: Introduction to the European Monitoring and Evaluation Programme
669 (EMEP) and observed atmospheric composition change during 1972–2009, *Atmos. Chem. Phys.*,
670 12(12), 5447–5481, doi:10.5194/acp-12-5447-2012, 2012.



671 Tranvik, L. J., Downing, J. A., Cotner, J. B., Loiselle, S. A., Striegl, R. G., Ballatore, T. J., Dillon, P.,
672 Finlay, K., Fortino, K. and Knoll, L. B.: Lakes and reservoirs as regulators of carbon cycling and
673 climate, *Limnol. Oceanogr.*, 54, 2298–2314, doi:10.4319/lo.2009.54.6_part_2.2298, 2009.

674 Vachon, D., Lapierre, J. and del Giorgio, P. A.: Seasonality of photochemical dissolved organic
675 carbon mineralization and its relative contribution to pelagic CO₂ production in northern lakes, *J.*
676 *Geophys. Res. Biogeosciences*, 121, doi:10.1002/2015JG003244, 2016.

677 Vähätalo, A. V. and Wetzel, R. G.: Long-term photochemical and microbial decomposition of
678 wetland-derived dissolved organic matter with alteration of ¹³C:¹²C mass ratio, *Limnol. Oceanogr.*,
679 53(4), 1387–1392, doi:10.4319/lo.2008.53.4.1387, 2008.

680 Vannote, R. L., Minshall, G. W., Cummins, K. W., Sedell, J. R. and Cushing, C. E.: The River
681 Continuum Concept, *Can. J. Fish. Aquat. Sci.*, 37(1), 130–137, doi:10.1139/f80-017, 1980.

682 Weishaar, J. L., Aiken, G. R., Bergamaschi, B. A., Fram, M. S., Fujii, R. and Mopper, K.: Evaluation
683 of specific ultraviolet absorbance as an indicator of the chemical composition and reactivity of
684 dissolved organic carbon., *Environ. Sci. Technol.*, 37, 4702–4708, doi:10.1021/es030360x, 2003.

685 Winterfeld, M., Goñi, M.A., Just, J., Hefter, J. and Mollenhauer, G.: Characterization of particulate
686 organic matter in the Lena River delta and adjacent nearshore zone, NE Siberia – Part 2: Lignin-
687 derived phenol compositions, *Biogeosciences*, 12, 2261–2283, 2015.

688

689

690

691

692

693

694



695 Table 1. Mean ($n=13 \pm 1$ standard deviation) water temperature and chemistry parameters including pH,
696 conductivity, POC concentrations, and FI values at the Black Burn and Loch Katrine.

	Black Burn	Loch Katrine
Water temperature °C	8.26 ± 4.53	10.9 ± 5.07
pH	5.38 ± 0.85	6.74 ± 0.32
Conductivity $\mu\text{S cm}^{-1}$	78.2 ± 30.7	25.2 ± 4.01
POC mg L^{-1}	5.78 ± 2.78	2.96 ± 0.63
FI value	1.15 ± 0.13	1.08 ± 0.18

697

698

699

700

701

702

703

704

705

706

707

708

709

710

711

712

713

714

715



716 Table 2. Pearson correlation coefficients between irradiation induced changes to aqueous carbon species and
 717 spectral properties, and water chemistry of Black Burn water samples from the year-long sampling campaign
 718 prior to irradiation and site conditions at Auchencorth Moss (n=13).

	Δ DOC	Δ DIC	Δ CO ₂	Δ CO	Δa_{254}	Δ E4:E6
DOC	0.708**	-0.074	0.773**	0.824**	0.766**	0.095
E4:E6	0.366	0.049	0.463	0.434	0.183	0.770**
SUVA ₂₅₄	0.228	0.460	0.232	0.129	0.231	-0.098
FI	-0.438	-0.161	-0.318	-0.238	-0.115	-0.485
Air temperature^a	-0.032	-0.379	-0.029	-0.052	0.220	-0.571*
Rainfall^b	0.603*	0.061	0.537	0.445	0.365	0.492
PAR^c	-0.161	-0.459	-0.380	-0.267	-0.224	-0.662*
Discharge^d	0.132	0.237	0.123	0.088	-0.139	0.767**

* p < 0.05
 ** p < 0.01
^a Mean monthly air temperature
^b Total monthly rainfall (mm)
^c Mean monthly PAR ($\mu\text{mol m}^{-1} \text{s}^{-1}$)
^d Mean monthly discharge (L s^{-1})

719

720

721

722

723

724

725

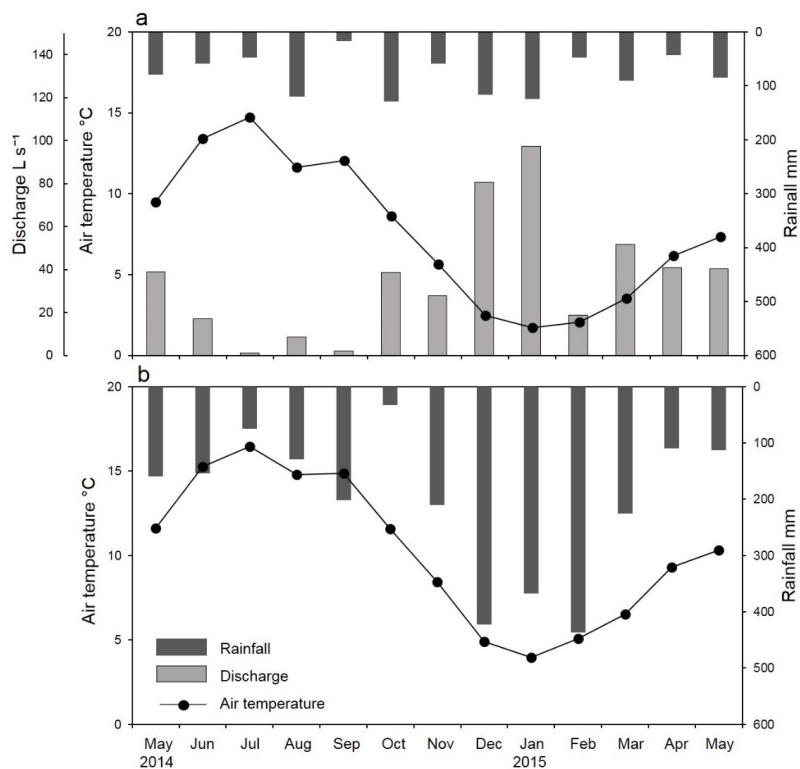
726

727

728



729 Figure 1. Mean monthly air temperature, total rainfall and mean discharge from May 2014 to May 2015 are
 730 shown for a) Auchencorth Moss, with discharge of the Black Burn shown on the left hand offset axis. Mean
 731 monthly air temperature and total rainfall are shown for the same period for Comer meteorological station, near
 732 Loch Katrine. Note inverted right hand y axes.



733

734

735

736

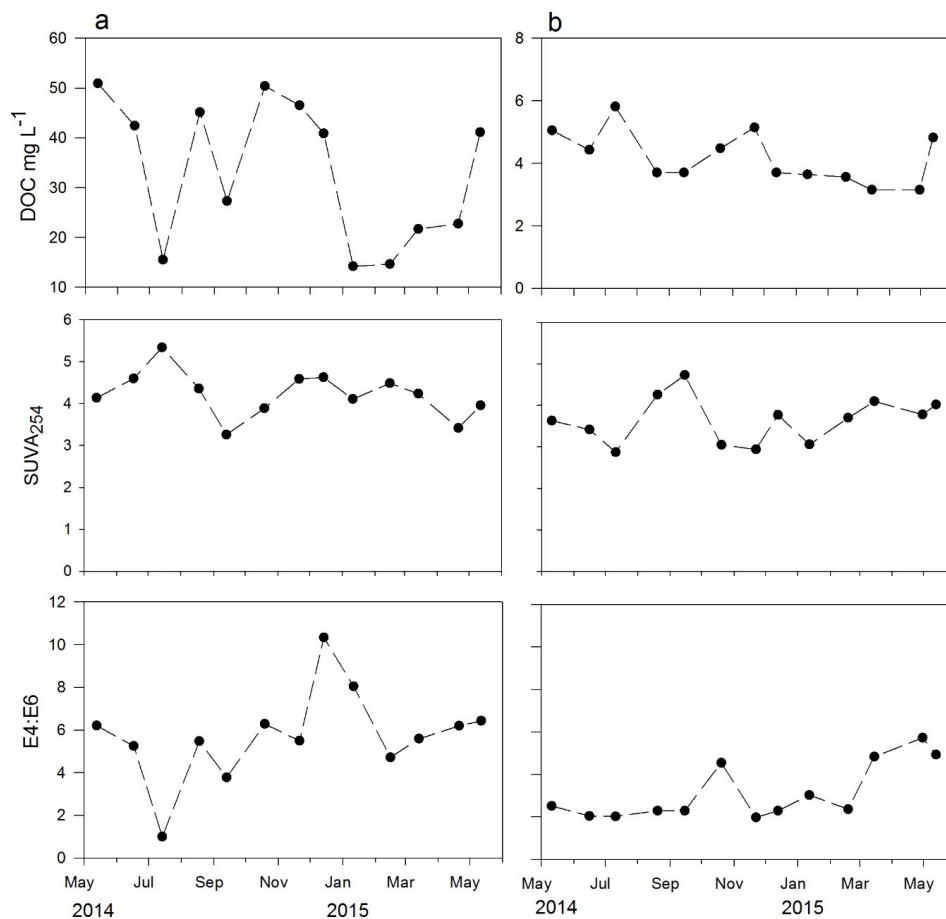
737

738

739



740 Figure 2. Time series at a) the Black Burn and b) Loch Katrine of DOC concentration and parameters for DOC
741 quality: SUVA₂₅₄ and E4:E6 from May 2014 to May 2015. Note different y axis scales for DOC data.



742

743

744

745

746

747

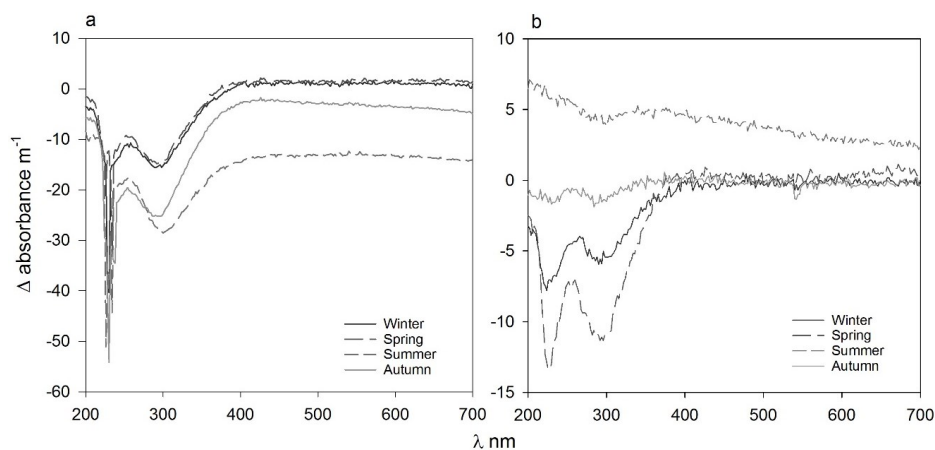
748

749



750 Figure 3. Irradiation induced changes (light exposed subtracted from dark controls) to water sample absorbance
 751 values at a) Black Burn and b) Loch Katrine. Summer is the mean of June, July and August values, autumn is
 752 the mean of September, October and November values, winter is the mean of December, January and February
 753 values and spring is the mean of March, April and the combined mean of May '14 and May '15 values. Note
 754 different y axis scales.

755



756

757

758

759

760

761

762

763

764

765

766

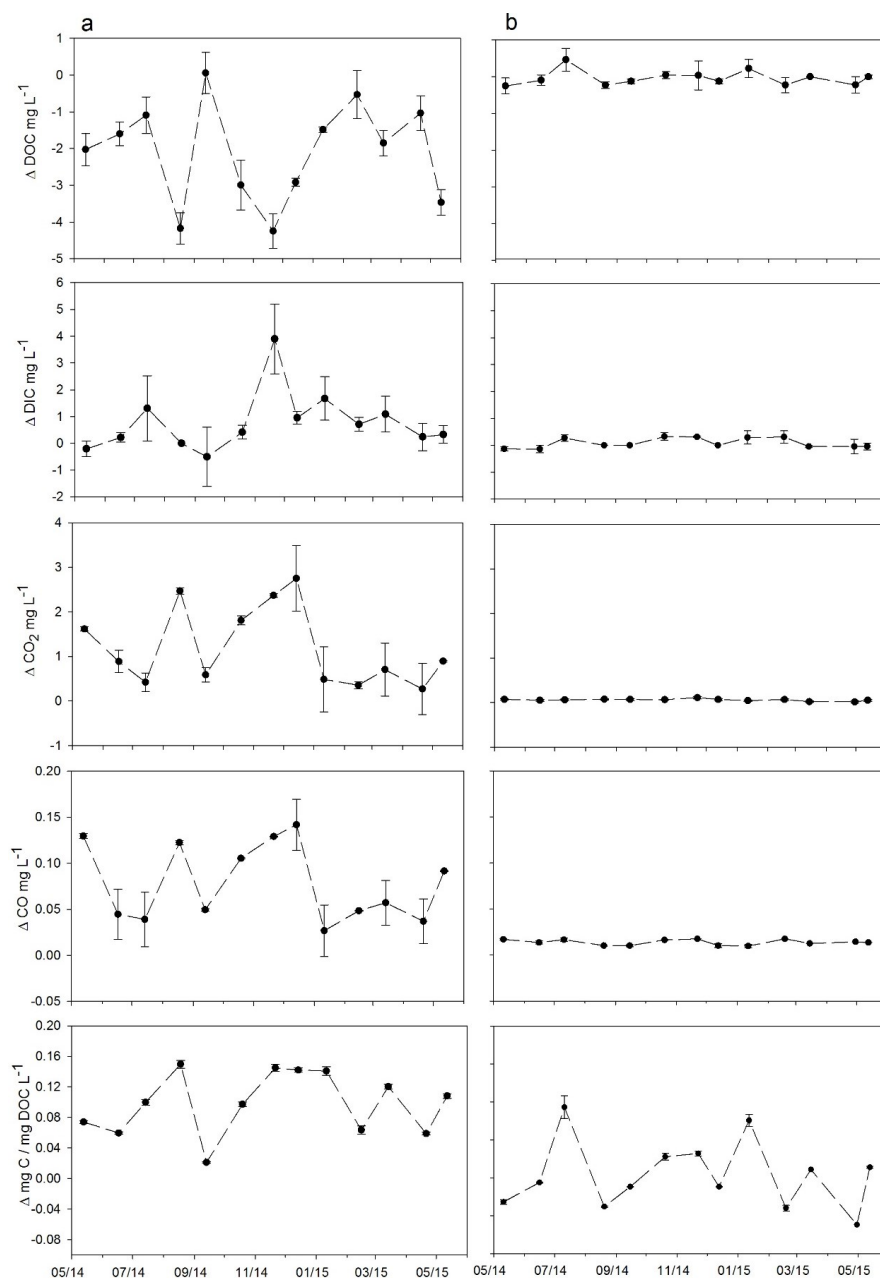
767

768



769 Figure 4. Irradiation induced changes to carbon species DOC, DIC, CO₂ and CO in monthly water samples from
770 panel Black Burn (panel a) and Loch Katrine (panel b). DOC normalised changes to all C species changes are
771 shown on the bottom row. Data represent the difference between the mean of irradiated and unirradiated control
772 samples. Error bars show the standard error of the mean (n=4).

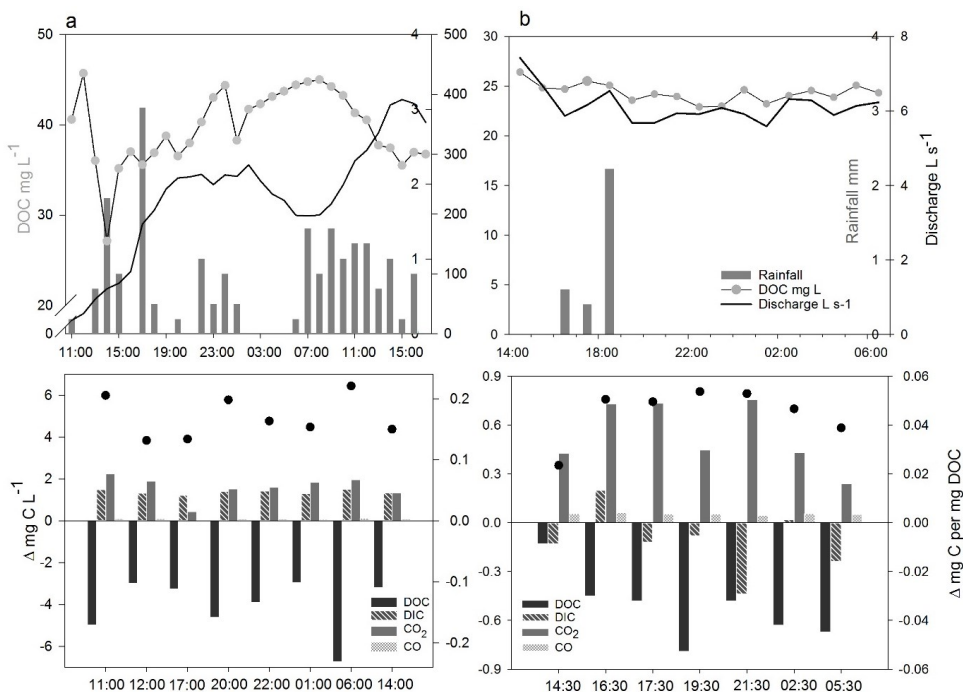
773



774



775 Figure 5. Rainfall events sampled on 9-10 December 2014 (panel a) and on 1-2 September 2015 (panel b). Row
 776 one shows a time series of hourly rainfall, discharge and DOC concentrations for each event. Row two shows
 777 photo-induced C pool changes of irradiated samples expressed as a total change value per C species in vertical
 778 bars (left y axis) and as a DOC normalised value in dots (right y axis). Data represent the difference between the
 779 mean of irradiated and unirradiated control samples (n=4). Note different x- and y-axis scales.



780

781

782

783

784

785

786

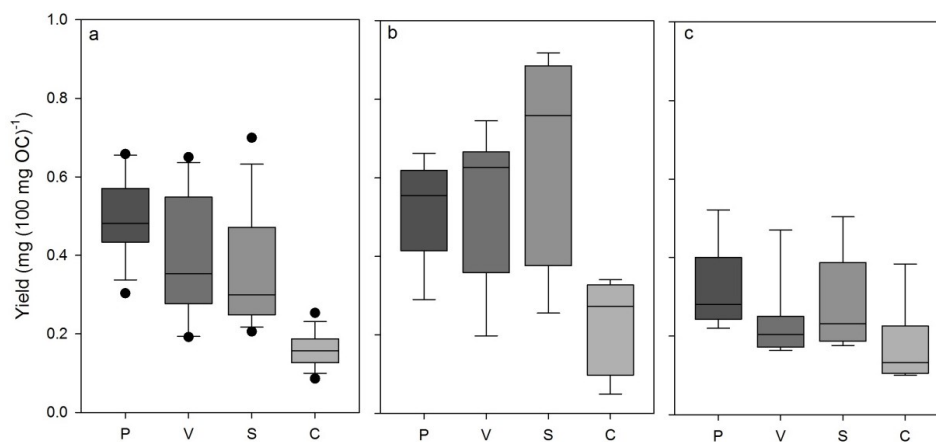
787

788

789



790 Figure 6. Boxplots of carbon-normalised yields of phenols groups for Black Burn water samples collected a)
791 monthly in the year-long study (n=13), b) during the winter rainfall event (n=8) and c) during the summer
792 rainfall event (n=7). P = p hydroxyl, V = vanillyl, S = syringyl and C = cinnamyl. The box spans from the first
793 quartile to the third quartile, with the line showing the median value. Whiskers show the minimum and
794 maximum values, with dots representing outlying values.



795

796

797

798

799

800

801

802

803

804

805

806

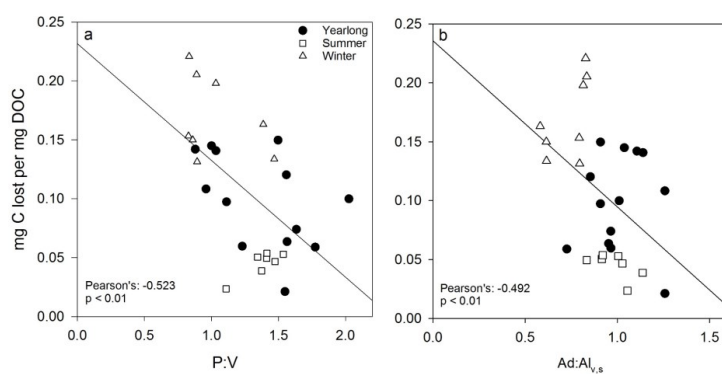
807

808

809



810 Figure 7. Pearson correlation between mg DOC lost upon irradiation per mg DOC and a) P:V ratios and b)
 811 Ad:Al_{v,s} (derived from acids and aldehydes from vanillyl and syringyl phenol groups) ratios in all Black Burn
 812 water samples analysed (n=28). Lines of best fit for all water samples are also shown. The monthly samples in
 813 the year-long study and the winter and summer rainfall event samples are indicated.



814

815

816